ORIGINAL ARTICLE

Cancer Science WILEY

Establishment and characterization of a novel cancer stem-like cell of cholangiocarcinoma

Orasa Panawan[1,2] | Atit Silsirivanit[1,2,3] | Chih-Hsiang Chang[1] | Siyaporn Putthisen[2] | Piyanard Boonnate[4] | Taro Yokota[1] | Yuki Nishisyama-Ikeda[1] | Marutpong Detarya[1,2,3] | Kanlayanee Sawanyawisuth[2,3] | Worasak Kaewkong[5] | Kanha Muisuk[6] | Sukanya Luang[2,3] | Kulthida Vaeteewoottacharn[2,3,4] | Ryusho Kariya[4] | Hiromu Yano[7] | Yoshihiro Komohara[7] | Kunimasa Ohta[8] | Seiji Okada[4] | Sopit Wongkham[2,9] | Norie Araki[1]

[1]Department of Tumor Genetics and Biology, Graduate School of Medical Sciences, Faculty of Life Sciences, Kumamoto University, Kumamoto, Japan

[2]Department of Biochemistry, Faculty of Medicine, Khon Kaen University, Khon Kaen, Thailand

[3]Cholangiocarcinoma Research Institute, Khon Kaen University, Khon Kaen, Thailand

[4]Division of Hematopoiesis, Joint Research Center for Human Retrovirus Infection, Kumamoto University, Kumamoto, Japan

[5]Department of Biochemistry, Faculty of Medical Sciences, Naresuan University, Phitsanulok, Thailand

[6]Department of Forensic Medicine, Faculty of Medicine, Khon Kaen University, Khon Kaen, Thailand

[7]Department of Cell Pathology, Faculty of Life Sciences, Kumamoto University, Kumamoto, Japan

[8]Department of Stem Cell Biology, Faculty of Arts and Science, Kyushu University, Fukuoka, Japan

[9]Center for Translational Medicine, Faculty of Medicine, Khon Kaen University, Khon Kaen, Thailand

Correspondence
Atit Silsirivanit, Department of Biochemistry, Faculty of Medicine, Khon Kaen University, Khon Kaen 40002, Thailand.
Email: atitsil@kku.ac.th

Norie Araki, Department of Tumor Genetics and Biology, Graduate School of Medical Sciences, Faculty of Life Sciences, Kumamoto University, Kumamoto 860-8556, Japan.
Email: nori@gpo.kumamoto-u.ac.jp

Abstract

Cholangiocarcinoma (CCA) is an aggressive malignant tumor of bile duct epithelia. Recent evidence suggests the impact of cancer stem cells (CSC) on the therapeutic resistance of CCA; however, the knowledge of CSC in CCA is limited due to the lack of a CSC model. In this study, we successfully established a stable sphere-forming CCA stem-like cell, KKU-055-CSC, from the original CCA cell line, KKU-055. The KKU-055-CSC exhibits CSC characteristics, including: (1) the ability to grow stably and withstand continuous passage for a long period of culture in the stem cell medium, (2) high expression of stem cell markers, (3) low responsiveness to standard chemotherapy drugs, (4) multilineage differentiation, and (5) faster and constant expansive tumor formation in xenograft mouse models. To identify the CCA-CSC-associated pathway, we have undertaken a global proteomics and functional cluster/network analysis. Proteomics identified the 5925 proteins in total, and the significantly upregulated proteins in CSC compared with FCS-induced differentiated CSC and its parental cells

[Corrections made on 05 July 2023, after first online publication: The 14th author's name and 18th author's affiliation have been corrected in this version.]

Abbreviations: 5-FU, 5-fluorouracil; ABC, ATP binding cassette; ALDH, aldehyde dehydrogenase; BRJ, BALB/c Rag-2null/Jak3null; CCA, cholangiocarcinoma; CSC, cancer stem cell; EpCAM, epithelial cell adhesion molecule; GEPIA, Gene Expression Profiling Interactive Analysis; HMGA1, high mobility group A1; PTS, phase-transfer surfactant; SC, sphere cell; SDC, sodium deoxycholate; SLS, sodium lauroyl sarcosinate; STAT3, signal transducer and activator of transcription 3; STR, short tandem repeat; TCGA, The Cancer Genome Atlas.

were extracted. Network analysis revealed that high mobility group A1 (HMGA1) and Aurora A signaling through the signal transducer and activator of transcription 3 pathways were enriched in KKU-055-CSC. Knockdown of HMGA1 in KKU-055-CSC suppressed the expression of stem cell markers, induced the differentiation followed by cell proliferation, and enhanced sensitivity to chemotherapy drugs including Aurora A inhibitors. In silico analysis indicated that the expression of HMGA1 was correlated with Aurora A expressions and poor survival of CCA patients. In conclusion, we have established a unique CCA stem-like cell model and identified the HMGA1-Aurora A signaling as an important pathway for CSC-CCA.

KEYWORDS
bile duct, cancer stem cell, cholangiocarcinoma, HMGA1, liver

1 | INTRODUCTION

Although CCA is considered a rare tumor, the number of cases and deaths is increasing worldwide.[1] The aggressive malignant phenotypes lead to a poor prognosis for CCA patients. Chemotherapy with gemcitabine, cisplatin, and 5-FU is necessary for patients with advanced and unresectable tumors.[2,3] However, chemoresistance and tumor recurrence remain significant problems in CCA patients.[4,5]

Cancer stem cells were reported as an important factor in promoting cancer progression, therapeutic resistance, and disease recurrence.[6,7] Targeting CSCs could be a promising strategy for achieving curative treatment.[7,8] Several in vitro and in vivo experimental protocols, such as tumor-sphere formation assay and cell sorting by flow cytometry, have been used to isolate and assess the cancer stem-like cells.[9,10] The isolated cells exhibited CSC phenotypes, such as drug resistance, multilineage differentiation, and in vivo tumor formation.[11,12] The sources of this minor but useful cell subpopulation could be either primary tumor tissues or the established cancer cell lines.[13–15]

The accumulated evidence suggests that the tumor tissue of CCA is rich in the CSC population and implicates CCAs as stem cell-based diseases.[16,17] However, the information regarding the biology of CSC in CCA is very limited due to the lack of CCA-CSC models to be characterized. In this study, a novel stable/long-life CCA stem-like cell, KKU-055-CSC, has been isolated from the established CCA cell line. In vitro and in vivo experiments revealed that the cells exhibit the features of CSCs, suggesting its potential to be a representative CSC clone for CCA. Using global proteomics and network analyses, we identify the CCA-CSC-associated pathways and their key molecules as candidates to be targeted. Functional and in silico studies were carried out to explore their role in CCA-CSC and determine their potential as a target for CCA treatment.

2 | MATERIALS AND METHODS

2.1 | Cell lines and cell culture

A parental CCA cell line, KKU-055, was established from poorly differentiated primary CCA tissue of a 56-year-old Thai man and was obtained from the Japanese Collection of Research Bioresources Cell Bank. The cell was maintained in DMEM (Thermo Fisher Scientific) supplemented with 10% FCS (MP Biomedicals). KKU-055 CCA stem-like cell (KKU-055-CSC) was maintained in a stem cell culture medium.[18] The CSCs were subcultured once a week using Accumax (Innovative Cell Technologies). All cell lines were cultured in an incubator at 37°C with 5% CO_2.

2.2 | Establishment of CCA stem-like cells from a CCA cell line

The CCA stem-like cell KKU-055-CSC was derived/reprogrammed from the adherent parental KKU-055 CCA cell line using protocols modified from previous reports.[13,18] Briefly, the parental KKU-055 cells were trypsinized and washed with PBS to remove the FCS. The cells were resuspended in a stem cell culture medium and seeded to form spheres in an ultralow attachment culture dish (Corning). Fibroblast growth factor, epidermal growth factor, and insulin were added every 2 days. Cells were continuously cultured and subpassaged carefully once a week for more than 3 months, more than 15 passages, to ensure that the cells formed spheres/spheroids stably during their culture. After 15 passages, the cells were stably cultured in the standard TC-treated cell culture dish (Falcon; Corning).

2.3 | Cell proliferation and drug sensitivity assays

For the proliferation assay, the KKU-055-CSC and parental KKU-055 cells were seeded in a 96-well plate at 1000 cells/100 μL/well. Cell number was measured from day 0 to day 3 using CCK-8 (Dojindo) as the manufacturer's recommendation. For the drug sensitivity assay, the cells were treated with the desired concentrations of 5-FU, cisplatin, gemcitabine, or Aurora A inhibitors. Phosphate-buffered saline (for gemcitabine) or equal DMSO concentration (for cisplatin, 5-FU, or Aurora A inhibitors) were used as the controls. After 72 h, the cell number was measured using CCK-8 (Dojindo). The relative cell viability was calculated as the percentage of viable cells in the treatment conditions compared with the control. Five replicates of each condition and three independent experiments were performed.

2.4 | Multilineage differentiation

Multilineage differentiation of KKU-055-CSC was analyzed as described previously.[18,19] Briefly, the cells were preseeded and allowed to form small spheres for 2 days. The differentiation was induced by treatment with 10% FCS, StemPro Osteogenesis, or StemPro Adipogenesis Differentiation media (Thermo Fisher Scientific). Alizarin Red S was used for calcium staining to confirm osteocyte differentiation. Adipocyte differentiation was identified by Oil Red O staining, which stains the lipid droplets in the cells.

2.5 | Western blot analysis

Cells were lysed using urea lysis buffer (8 M urea, 2 M thiourea, and 0.5 mM NaCl) and PTS solution (12 mM SDC, 12 mM SLS), in 100 mM Tris-HCl (pH 9) containing protease and phosphatase inhibitors (Roche Diagnostics). The SDS-PAGE and western blot analysis were carried out as previously described using the desired concentrations of primary Abs (Table S1).[18,20]

2.6 | Immunocytochemistry staining

Cells were seeded in a 24-well plate (2×10^4 cells/well) and cultured for 72 h. After complete incubation, the cells were washed twice with PBS and fixed in 90% cold methanol for 15 min. The cells were incubated with 1% BSA for 1 h to block nonspecific reactivity, followed by overnight incubation with the desired concentration of primary Abs at 4°C. The staining signal was detected by Alexa-547-conjugated anti-mouse or Alexa 488-conjugated anti-rabbit Abs; DAPI diluted 1:1000 (Invitrogen) was used for nuclear staining.

2.7 | RNA extraction and RT-PCR

Total RNA was extracted using the RNeasy Mini kit (Vivantis Technology). Two micrograms of total RNA was used for cDNA synthesis by a high-capacity cDNA Reverse Transcription kit (Applied Biosystems) according to the manufacturer's recommendation. The converted cDNA was diluted with nuclease-free water to obtain a final concentration of 20 ng/μL and used as the template for real-time PCR as previously described.[18] All primers are listed in Table S2.

2.8 | In vivo tumor transplantation

The in vivo experiments were carried out using BRJ mice[21] under the guidelines of the Animal Experiment Committee of Kumamoto University. The KKU-055-CSC or parental KKU-055 cells were injected subcutaneously into 8–12-week-old BRJ mice with varying cell numbers: Group 1, 3×10^5 cells/nodule and 1×10^6 cells/nodule, and Group 2, 3×10^4 cells/nodule and 1×10^5 cells/nodule. Five replicate experiments were carried out in each group. The animal conditions were monitored daily. Tumor volume (V) was calculated from length (L, the long part of the tumor) and width (W, the short part of the tumor) using the formula: $V = (W^2 \times L) / 2$.

The tumors were harvested and weighed when the diameter reached 2 cm at most in the group of xenografts.

2.9 | Immunohistochemistry of tumors from mouse xenografts

Tumor samples were fixed in 4% paraformaldehyde in PBS, embedded in paraffin, and cut into 4 μm sections; H&E staining was carried out to check the cell morphology in the tumor. For immunostaining, the sections were deparaffinized using xylene and rehydrated with a graded series of ethanol. Antigen retrieval was undertaken by heat-induced epitope retrieval in citrate buffer. The sections were incubated with 1% BSA in TBS for blocking, and stained with primary Abs against EpCAM (N1554; Dako), and Ki-67 (M7240; Dako). The sections were incubated with HRP-conjugated anti-mouse secondary Abs (Nichirei). Positive signals were visualized using diaminobenzidine (Nichirei).

2.10 | siRNA treatment

The siRNA against HMGA1 (siHMGA1; Ambion/Invitrogen) was transfected into KKU-055-CSC using an electroporation system. The 2×10^5 cells were resuspended in 10 μL serum-free Opti-MEM (Thermo Fisher Scientific) containing 50 pmole of siHMGA1. The electroporation was carried out by pulsing 1100 V, 30

pulse-width, twice in a MicroPorator MP-100 (Digital Bio; Thermo Fisher Scientific) using 10 μL Neon tips (Ambion/Invitrogen). After electroporation, the cells were cultured for 48–72 h. The siHMGA1 sequences were GUGCCAACACCUAAGAGACCUTT (sense) and AGGUCUCUUAGGUGUUGGCACTT (antisense).[22] Cells were treated with Silencer Negative Control siRNA (Ambion/Invitrogen) as a control siRNA (siControl).

2.11 | Cytogenetic and karyotype analysis

Parental KKU-055 and KKU-055-CSC cells were subjected to a conventional chromosomal analysis as in the protocol previously described.[3] Briefly, after the fixation, the chromosomes in the cells were trypsin-Giemsa-banded to identify individual metaphase chromosomes. Representative nonoverlapped chromosome figures were imaged. The karyotype analysis was based on criteria of the International System for Human Cytogenetic Nomenclature (ISCN).[23] The modal chromosome number was determined in at least 20 cells from each parental KKU-055 and KKU-055-CSC.

2.12 | Short tandem repeat analysis

The DNAs from KKU-055-CSC and parental KKU-055 cells were extracted using the genomic extraction kit (Qiagen). A standard STR profile was obtained with 15 loci and the gender marker (amelogenin), amplified using the AmplFLSTR PCR Amplification kit and analyzed by 3130xl Genetic Analyzer (Applied Biosystems). Obtained data were analyzed using the GeneMapper ID-X Software version 1.4 (Applied Biosystems).

2.13 | Proteomic analysis

The parental KKU-055, KKU-055-CSC, and 10% FCS-induced differentiation form (KKU-055-DIF) were cultured for 72 h. The cellular proteins were prepared according to the previously described protocol.[24] Briefly, the cell lysate was harvested using PTS lysis buffer (12 mM SDC, 12 mM SLS), in 100 mM Tris buffer (pH 9) containing protease inhibitor cocktails (Sigma-Aldrich). The cell lysates (400 μg each) were digested with Lys-C (Wako Chemicals) and trypsin (MS grade; Promega). Four replicate samples were prepared for each group. The liquid chromatography–tandem mass spectrometry analyses were carried out using an Orbitrap Fusion Tribrid mass spectrometer (Thermo Fisher Scientific) connected with an EASY-nLC 1200 (Thermo Fisher Scientific). Mass spectrometry data were processed and searched against the UniProtKB/SwissProt (2021_09) human database using Protein Discoverer 2.4. The detailed protocol for proteomic analysis is described in Data S1. The mass spectrometry data are available in the Japan ProteOme STandard (jPOST) Database (accession nos. JPST002032, PXD039953).[25]

2.14 | Statical analysis

For functional assays, the statistical analyses and graph construction were carried out using GraphPad Prism 9.0 software (GraphPad Software). Data are presented as the mean ± SD. Student's t-test was used to compare the data between groups; *$p < 0.05$ and **$p < 0.01$ were considered statistically significant. The statistical analysis of proteomics is described in Data S1.

3 | RESULTS

3.1 | Cholangiocarcinoma stem-like cell KKU-055-SC was established from the KKU-055 CCA cell line

To establish the CCA stem-like cell, the parental KKU-055 CCA cells were seeded onto an ultralow attachment culture dish and continuously cultured in a stem cell culture medium. The cells could form floating 3D clusters, continuously growing and long-term serial subpassaged. After subpassage, reformation of the small spheres (<20 μm) could be observed within 48 h and continuously enlarged to reach approximately 100 μm within 7 days (Figure 1A). After 3 months, the cells could propagate as a floating sphere without attaching to the standard TC-treated cell culture dishes. Over the past 3 years, the cells could be serial subpassaged and constantly reformed the spheres for more than 100 passages. Typically, the cells were kept at −80°C in the stem cell banker by checking the stem cell phenotypes after 20–30 passages. All experiments were carried out with those stock cells and finished within 20 passages. As the cells can maintain their ability to form spheres constantly, we first named these cells KKU-055-SC.

To validate whether KKU-055-SC showed stem cell characteristics in general, we examined the expression of stem cell markers in the sphere form of KKU-055-SCs compared with parental KKU-055 cells. Western blotting showed that the reported CCA stem markers (SOX2, CD44, CD147, and EpCAM) were highly expressed in KKU-055-SCs, whereas less expressed or undetectable in parental KKU-055 cells (Figure 1B). High expression of SOX2, CD44, EpCAM, and CD44v9 in KKU-055-SCs was also demonstrated by immunofluorescence staining (Figure 1C). In addition, real-time RT-PCR indicated that KKU-055-SCs express higher mRNA levels of SOX2, Oct3/4, c-myc, OLG2, CD44, and EpCAM compared with parental cells (Figure 1D). [Corrections made on 05 July 2023, after first online publication: "KKU-055-CSC" was corrected to "KKU-055-SC" in the heading for Section 3.1].

3.2 | KKU-055-SCs show stem cell phenotypes

3.2.1 | Cellular proliferation

The CSC is generally defined as a quiescent cell with a low proliferative rate, although it possesses a high tumorigenic ability. Cell
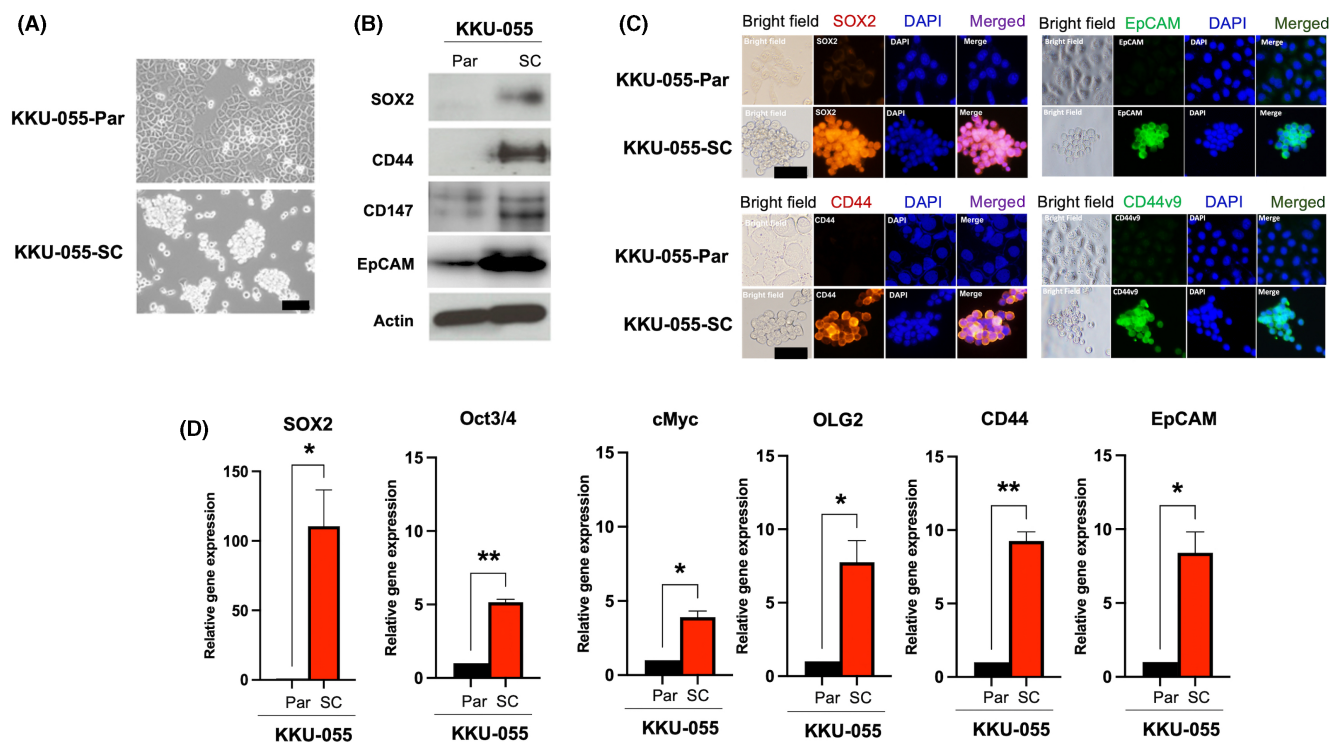
FIGURE 1 Morphology and stem cell marker expression. (A) Phase contrast of parental KKU-055 cells (KKU-055-Par) and KKU-055 sphere cells (KKU-055-SC; 50th passage). Scale bar, 50 μm. (B) Expression of SOX2, CD44, CD147, and epithelial cell adhesion molecule (EpCAM) was determined by western blot analysis. (C) Immunocytofluorescence was used to assess the expression of SOX2, EpCAM, CD44, and CD44v9. DAPI was used for nuclear staining. (D) Real-time RT-PCR was used to quantify the mRNA expression of *Sox2*, *Oct 3/4*, *C-myc*, *OLG-2*, *CD44*, and *EpCAM*. β-Actin was used as an internal control for normalization. $*p < 0.05$, $**p < 0.01$.

proliferation assay using CCK-8 (Dojindo) showed that KKU-055-SCs exhibited a significantly lower proliferation rate than parental KKU-055 cells (Figure 2A).

3.2.2 | Sensitivity against anticancer drugs

Another important CSC property is the gain of chemoresistance; therefore, we have analyzed the sensitivities of KKU-055-SCs against standard chemotherapeutic drugs for CCA treatment. Compared with parental KKU-055 cells, KKU-055-SC showed higher resistance to cisplatin, 5-FU, and gemcitabine (Figure 2B). The IC_{50} value at 72h of cisplatin in KKU-055-SC (6.3 μM) was significantly higher than parental cells (2.0 μM). For 5-FU, the IC_{50} value in KKU-055-SC was 31.6 μM, which is significantly higher than that of parental KKU-055 cells (19.9 μM). The IC_{50} value of gemcitabine in KKU-055-SC was higher than 25 nM, while in parental KKU-055 cells the value was 15.4 nM.

3.2.3 | Multilineage differentiation

To demonstrate the differentiating ability of KKU-055-SC, the cells were treated with FCS and specific differentiation media. After treatment with 10% FCS for 72h, KKU-055-SC became adherent cells resembling parental cells (Figure 2C). Moreover, the KKU-055-SCs

could differentiate into adipocytes and osteocytes by adipogenesis and osteogenesis differentiation media, respectively, after 14 days. Lipid droplet accumulation in the cytoplasm of the induced adipocytes was shown by positive staining with Oil Red O. The osteocyte differentiation was confirmed with calcium staining by Alizarin Red.

3.2.4 | Tumor initiation ability in mouse transplantation model

Xenotransplantation in a mouse model was used to evaluate the tumorigenicity of KKU-055-SC. Varying numbers of KKU-055-SC and parental KKU-055 cells were subcutaneously injected into BRJ mice as the workflow in Figure 3A. The ability in tumor formation of KKU-055-SC was significantly higher than parental KKU-055 (Figure 3B–D). At week 4, tumors were observed in mice injected with 3×10^5 and 1×10^6 cells/nodule. The mice were then killed and the tumors were excised on day 31. With 1×10^6 cells/nodule, the weight of tumors formed from KKU-055-SC was 0.84 ± 0.24 g, while that from parental KKU-055 cells was 0.14 ± 0.05 g (Figure 3E). With 3×10^5 cells/nodule, the weight of tumors formed from KKU-055-SC was 0.39 ± 0.26 g, while that by parental KKU-055 cells was 0.11 ± 0.06 g. At week 5, the tumor nodules transplanted with 1×10^5 KKU-055-SCs were observed and allowed to grow until they reached a 2 cm diameter on day 46 (approximately 6.5 weeks). Of those transplanted with 1×10^5 cells/
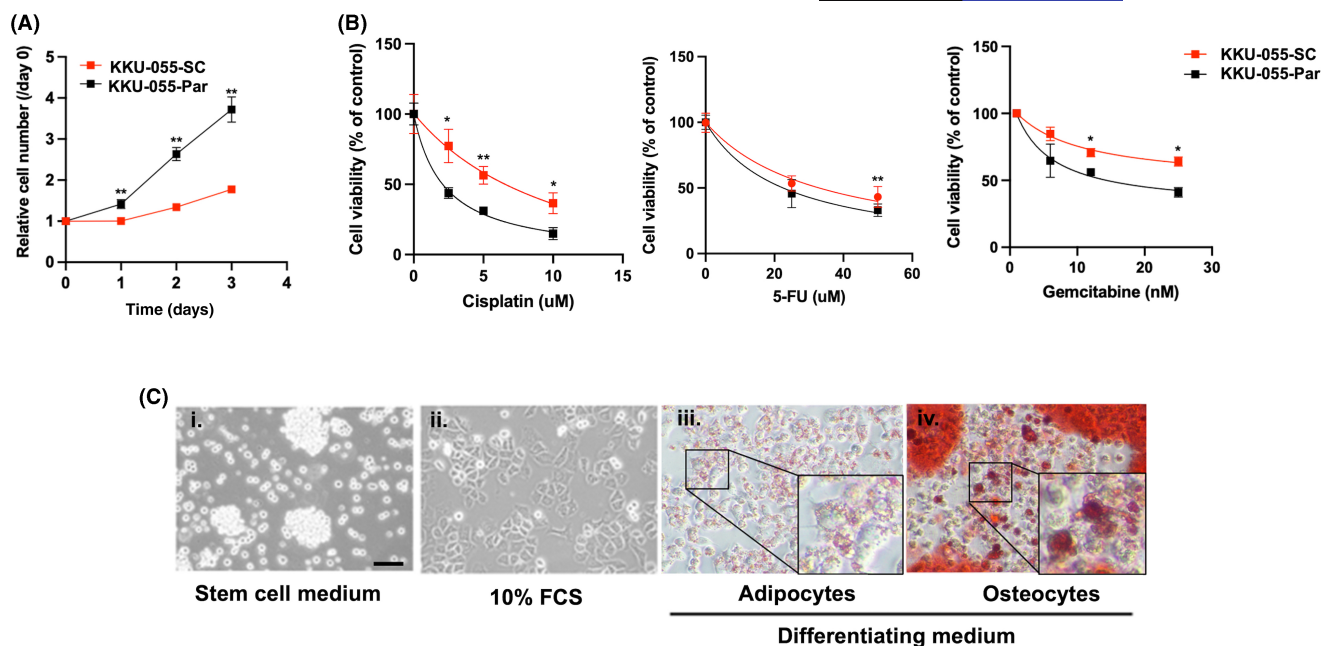
FIGURE 2 Phenotypic characteristics of KKU-055 sphere cells (KKU-055-SC) and parental KKU-055 cells (KKU-055-Par). (A) Proliferation of KKU-055-SC was compared with parental KKU-055 cells using CCK-8. (B) Dose–response curves represented cell viability 72 h after treatment with cisplatin, 5-fluorouracil (5-FU), and gemcitabine. *$p < 0.05$, **$p < 0.01$. (C) Morphology of KKU-055-SC in (i) stem cell medium. Multi-lineage differentiation ability was determined by (ii) 10% FCS-induced differentiation for 72 h, (iii) Oil Red O staining of fat droplets (red) after adipocyte differentiation, and (iv) Alizarin Red S staining of calcium granule (red) after osteocyte differentiation. Scale bar, 50 μm.

nodule, the tumor weight of KKU-055-SC was 0.57 ± 0.32 g, and that of parental KKU-055 was 0.13 ± 0.08 g. The immunohistochemistry showed that all tumors arising from KKU-055-SC showed a stronger positive signal of proliferative marker Ki-67 and CCA stem cell marker EpCAM compared with those of parental KKU-055 cells (Figure 3F). These results indicated that KKU-055-SC possesses higher in vivo tumorigenicity compared with the parental KKU-055 cancer cell line.

Collectively, our CCA sphere cells exhibited cancer stem cell phenotypes, including stem cell marker expression, self-renewal, drug resistance, multilineage differentiation, and higher tumor formation ability. Therefore, we defined the KKU-055-SC as a CCA stem-like cell and renamed it KKU-055-CSC.

3.3 | KKU-055-CSC showed identical chromosome phenotypes to parental KKU-055 cell line

Karyotype analysis revealed that KKU-055-CSCs and parental KKU-055 cells exhibit similar aneuploidy karyotypes with marked structural abnormalities of the chromosomes. The representative G-banded karyotypes are shown in Figure 4. The numbers of chromosomes among 20 examined cells were illustrated as an equal modal chromosome number of 54 of parental KKU-055 cells and KKU-055-CSCs. To verify the cell origin, STR analysis was carried out to compare with the information provided in the Japanese Collection of Research Bioresources (https://cellbank.nibiohn.go.jp/~cellbank/en/search_res_det.cgi?ID=7070). As shown in

Table 1, the STR profiles of the KKU-055-CSCs were more than 95% similar to those of the parental KKU-055 cells and original patient tissue, supporting the exact origin of the KKU-055-CSCs and parental KKU-055 cells. In addition, after long-term passages over 3 years, the KKU-055-CSCs have not changed their chromosomal phenotypes.

3.4 | Proteome profiling differentially expressed in KKU-055-CSC, compared with KKU-055-DIF and KKU-055 parental cells

To explore the molecular characteristics of CSC, we carried out global proteomics to compare KKU-055-CSC with KKU-055-DIF and the parental KKU-055. Four biological replicated samples from KKU-055-CSC, KKU-055-DIF, and parental KKU-055 cells were prepared and subjected to proteomics analysis, shown as a workflow in Figure 5A. The global label-free quantification proteomics identified 42,706 unique peptides corresponding to 5925 proteins (false discovery rate <1%). Pearson correlation showed that the identified proteins were highly correlated among the biological quadruplicates (Figure S1). Hierarchical clustering analysis was carried out to illustrate an overview of the global proteome changes arising between the three different stages of the cells (Figure 5B). Cluster analysis showed that proteome profiles of CSC are closer to that of DIF than that of the parental cell line. The k-mean clustering revealed five discrete protein expression patterns (Figure 5B,C).
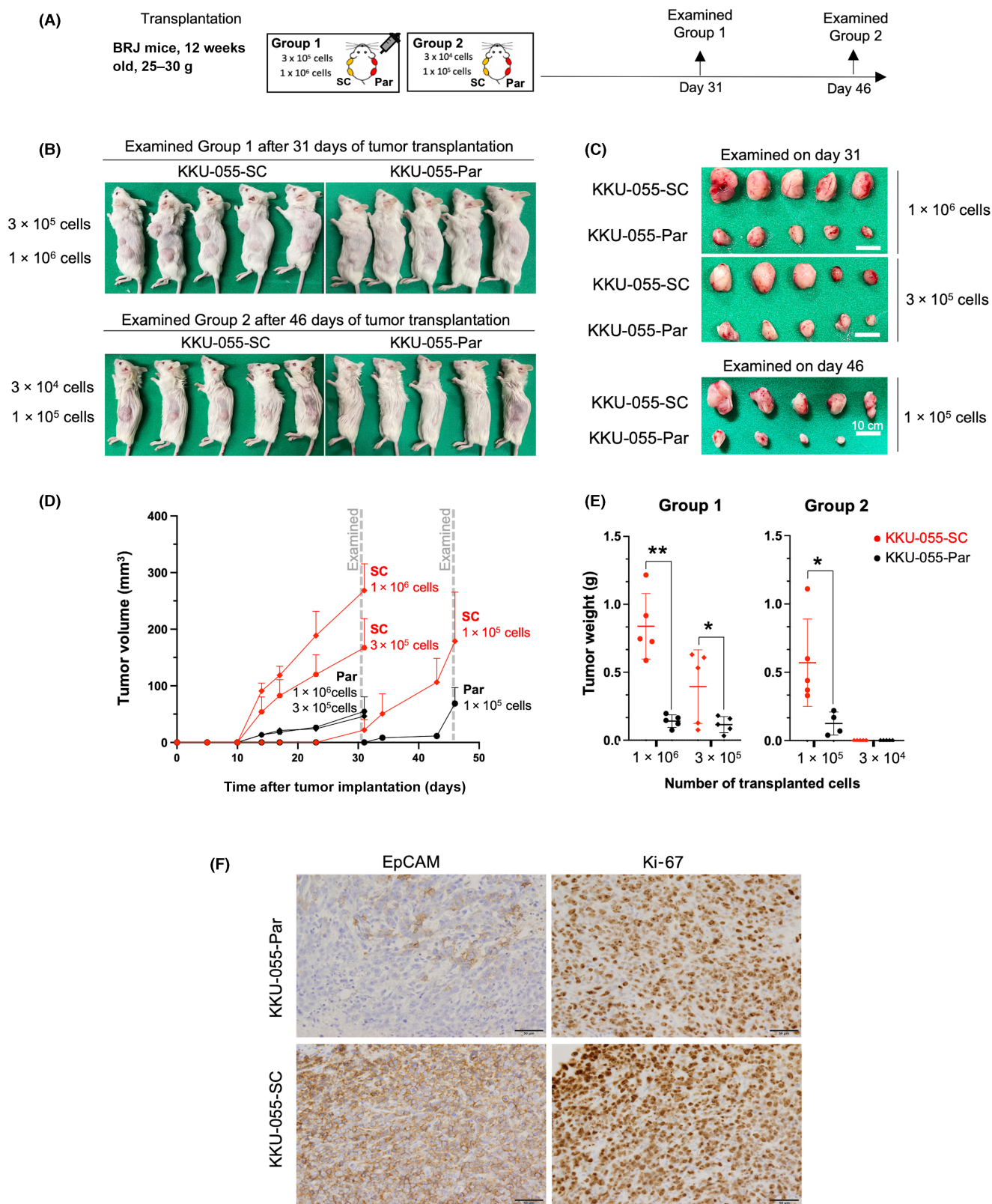
FIGURE 3 Tumor-initiating ability of KKU-055 sphere cells (KKU-055-SCs) in a mouse model. (A) Schematic diagram represents the workflow of tumor transplantation in the mouse model. (B, C) Tumors were presented in experimental animals and were harvested on day 31 and day 46. (D) Tumor size was measured daily, and (E) weight was measured after harvesting. (F) Harvested tumors were immunohistochemically stained by a proliferative index, Ki-67, and a stem marker, epithelial cell adhesion molecule (EpCAM). The signal was developed by diaminobenzidine (brown). Scale bar, 50 μm. *$p < 0.05$, **$p < 0.01$. KKU-055-Par, parental KKU-055.
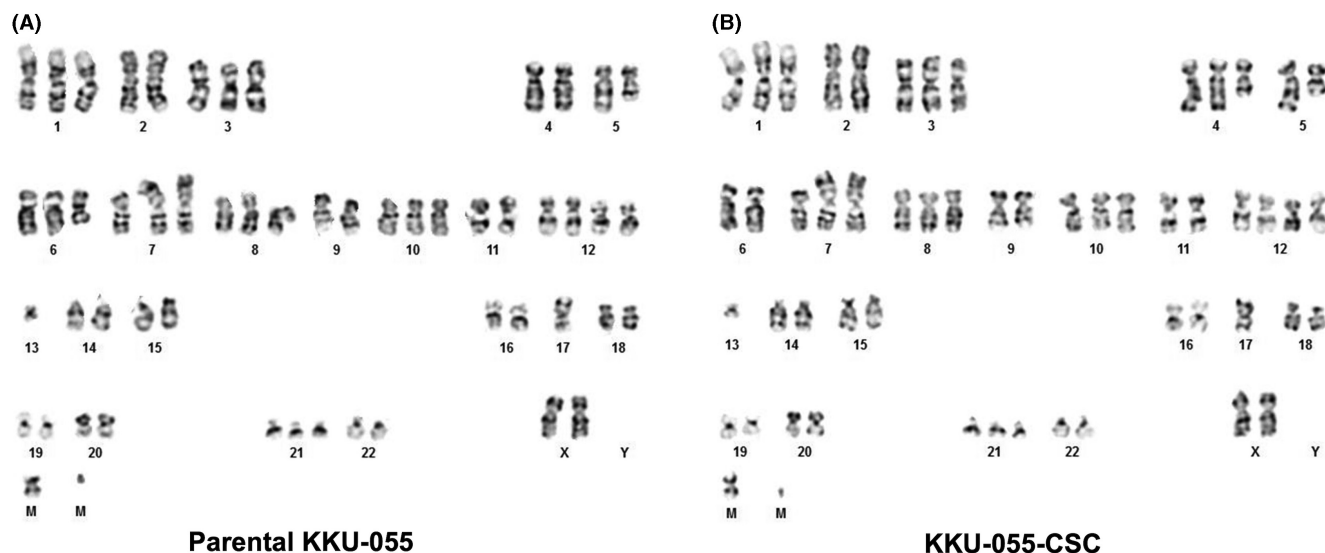
FIGURE 4 Karyotype analysis. Chromosome analysis of (A) parental KKU-055 cells (KKU-055-Par) and (B) cholangiocarcinoma stem-like cells (KKU-055-CSC) was carried out by G-band karyotyping. The chromosome images are representative of 20 examined mitotic cells. There was an equal modal chromosome number of 54 (53–56 chromosomes of KKU-055-Par cells and 52–55 chromosomes of KKU-055-CSCs). Several chromosome markers (M, mar) were similar in both, such as for parental KKU-055: 53+XX; +1, +3, +6, +7, +8, +10, +12, −13, −17, +21, +mar and for KKU-055-CSC: 53+XX; +1, +3, +4, +7, +8, +10, +12, −13, −17, +21, +mar.

TABLE 1 Short tandem repeat profiles of cholangiocarcinoma KKU-055 cells and KKU-055 stem-like cells (KKU-055-CSC)

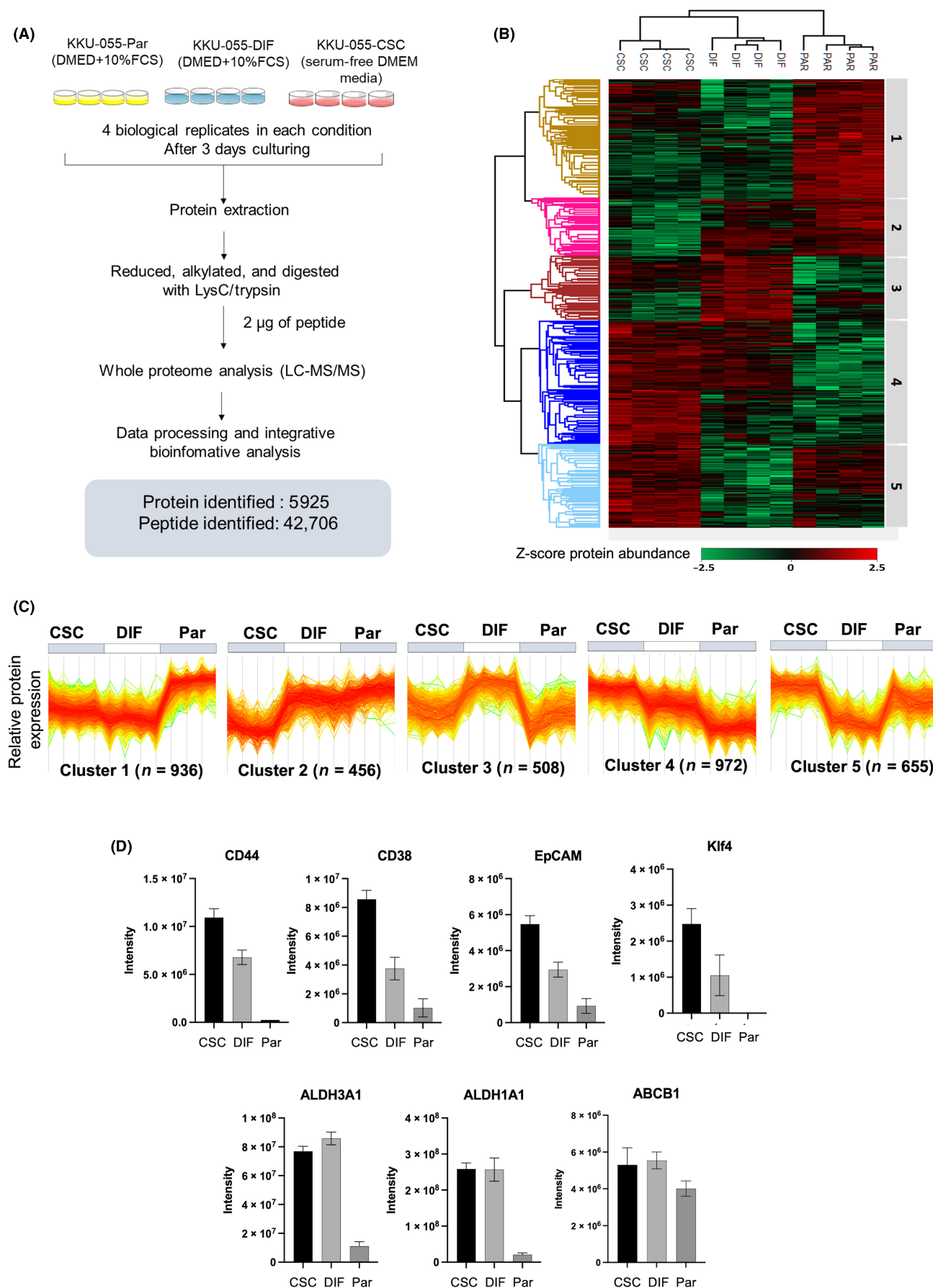| Locus	KKU-055 (JCRB1551)	Parental KKU-055	KKU-055-CSC
D8S1179	ND	14, 16, 17	14, 16, 17
D21S11	ND	29, 31	29, 31
D7S820	7, 8	7, 8	7, 8
CSF1PO	10, 11	10, 11	10, 11
D3S1358	ND	16, 17	16, 17
TH01	9, 9	9, 9	9, 9
D13S317	11, 11	11, 11	11, 11
D16S539	10,13	10, 13	10, 13
D2S1338	ND	22, 22	22, 22
D19S433	ND	14, 14	14, 14
vWA	17, 19	17, 19	17, 19
TPOX	8, 8	8, 8	8, 8
D18S51	ND	16, 17	16, 17
D5S818	11, 11	11, 11	11, 11
FGA	ND	26, 26	25, 26
Amelogenin	X	X	X

Abbreviations: JCRB, Japanese Collection of Research Bioresources; ND, Not determine; X, Chromosome X.
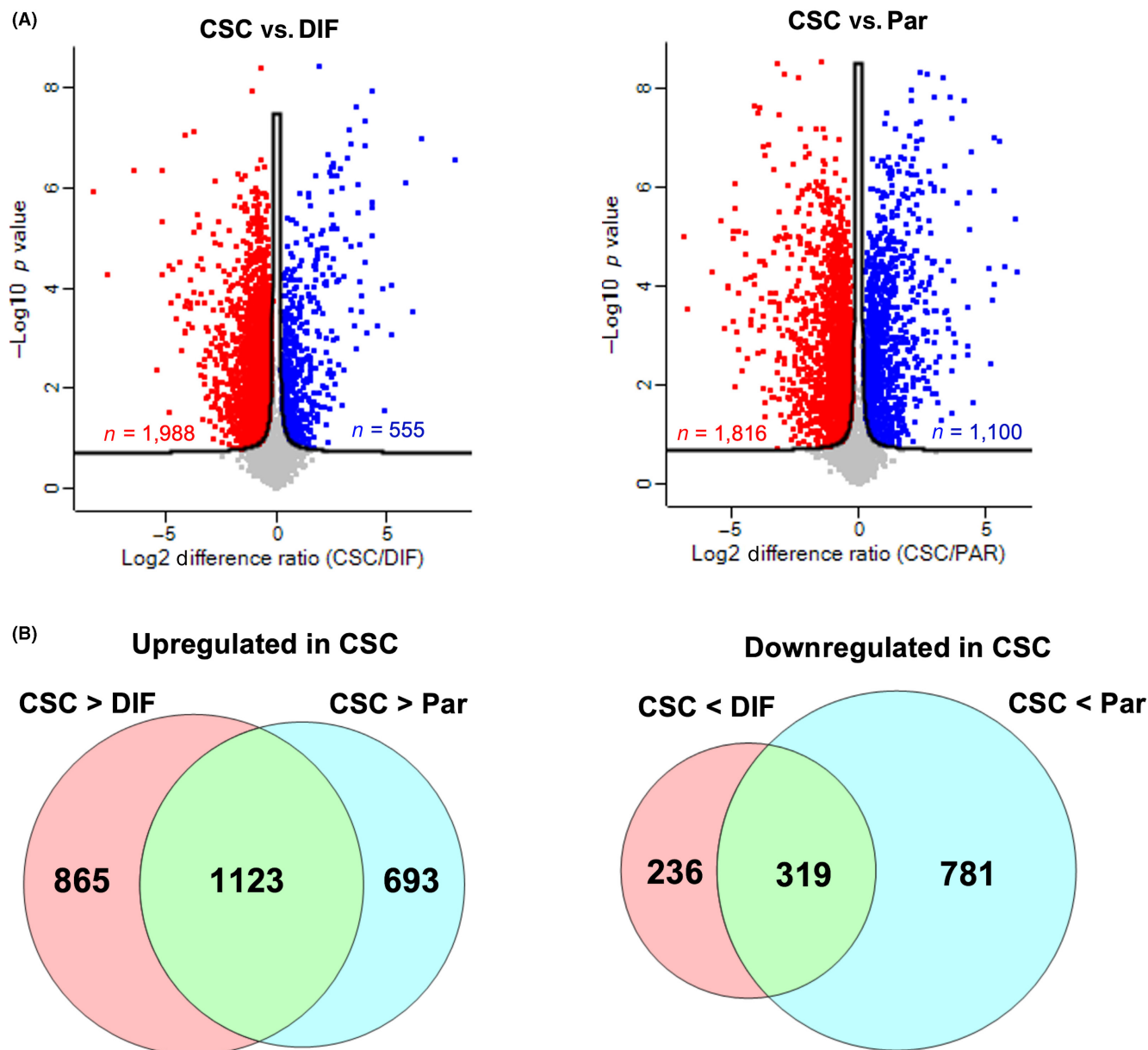
Clusters 1 and 2 represented the 936 and 456 proteins, of which expression was low in CSC, increased upon differentiation, and maintained at a high level in parental cells. Cluster 3 is a group of proteins ($n = 508$) highly expressed in the differentiation stage but low in CSC and parental cells. Cluster 4 contained 972 proteins highly expressed in CSC but low in the differentiation stage and parental cells. Cluster 5 is the group of proteins ($n = 655$) highly expressed in CSC and parental cells but low in the differentiation stage. From our proteomics data, the stem cell markers (CD44, CD38, EpCAM, Kif4) and multidrug resistance proteins (ALDH3A1, ALDH1A1, and ABCB1) were highly detected in KKU-055-CSC, as they are categorized in Cluster 4 (Figure 5D). These CSC-associated proteins are gradually downregulated during differentiation and totally lost or significantly reduced in the parental cells, suggesting that KKU-055-DIF could be represent an intermediate stage in the transition from stem cells to parental cancer cells.

3.5 | Network analyses of proteins significantly expressed in KKU-055-CSC

The volcano plots were used to compare the proteome profiles of KKU-055-CSC with KKU-055-DIF and parental KKU-055 (Figure 6A). We identified 1988 upregulated and 555 downregulated

FIGURE 5 Proteomics of cholangiocarcinoma stem-like cells (KKU-055-CSC), the 10% FCS-induced differentiation form (KKU-055-DIF), and parental KKU-055 (KKU-055-Par) cells. (A) Schematic diagram representing the proteomics workflow. (B) Cluster analysis of the quantitatively identified proteins. (C) k-mean clustering (D) The target stem cell markers' expression level, represented by mass intensity, was extracted from cluster 4 of the identified proteins. ABC, ATP binding cassette; ALDH, aldehyde dehydrogenase; EpCAM, epithelial cell adhesion molecule; LC-MS/MS, liquid chromatography–tandem mass spectrometry.

(A)

KKU-055-Par (DMED+10%FCS) KKU-055-DIF (DMED+10%FCS) KKU-055-CSC (serum-free DMEM media)

4 biological replicates in each condition
After 3 days culturing

Protein extraction

Reduced, alkylated, and digested with LysC/trypsin

2 µg of peptide

Whole proteome analysis (LC-MS/MS)

Data processing and integrative bioinfomative analysis

Protein identified : 5925
Peptide identified: 42,706

(B)

Z-score protein abundance
−2.5   0   2.5

(C)

Cluster 1 (*n* = 936)   Cluster 2 (*n* = 456)   Cluster 3 (*n* = 508)   Cluster 4 (*n* = 972)   Cluster 5 (*n* = 655)

(D)

CD44   CD38   EpCAM   Klf4

ALDH3A1   ALDH1A1   ABCB1

(A)

(B)

FIGURE 6 Differentially expressed proteins among cholangiocarcinoma stem-like cells (CSC), the 10% FCS-induced differentiation form (DIF), and parental (Par) KKU-055 cells. (A) Volcano plots represent differentially expressed proteins. Red dots represent proteins significantly upregulated in CSC. Blue dots represent proteins significantly upregulated in KKU-055-DIF and parental KKU-055 cells. (B) Venn diagram of proteins upregulated or downregulated in CSC, compared with DIF and Par cells. Numbers represent the number of proteins.

proteins in KKU-055-CSC compared with KKU-055-DIF, with 1816 proteins upregulated and 1100 proteins downregulated compared with parental KKU-055. After merging the data, we found 1123 and 319 proteins were specifically upregulated and downregulated, respectively, in KKU-055-CSC (Figure 6B, Tables S3–S5). These upregulated and downregulated proteins were further subjected to pathway analysis using KeyMolnet software. As a result, the top 20 and 10 overrepresentative pathways were identified and are listed in Table 2.

The network analysis was undertaken to identify the CCA-CSC-associated signaling pathway, focusing on upregulated proteins in

CSC. Using the KeyMolnet network search algorithm "start points and end points", the 1123 upregulated proteins were set as the "start point" and the cancer stem cell pathway was set as the "end point". The results revealed a complex network of targets with the most statistically significant relationships (Figure 7A). We extracted a specific network focusing on the HMGA1-STAT3-Aurora A pathway in the highly enriched pathways, showing the highest expression in CSC and regulating many molecules in the center of this network (Figure 7B). The CSC-specific expressions of those molecules that make up this network, such as HMGA1, STAT3, Aurora A, CD44, BRG, and SWI/SNF-related proteins, were confirmed in

TABLE 2 Pathways enriched from KKU-O55 stem-like cell (KKU-055-CSC) upregulated and downregulated proteins using KeyMolnet software

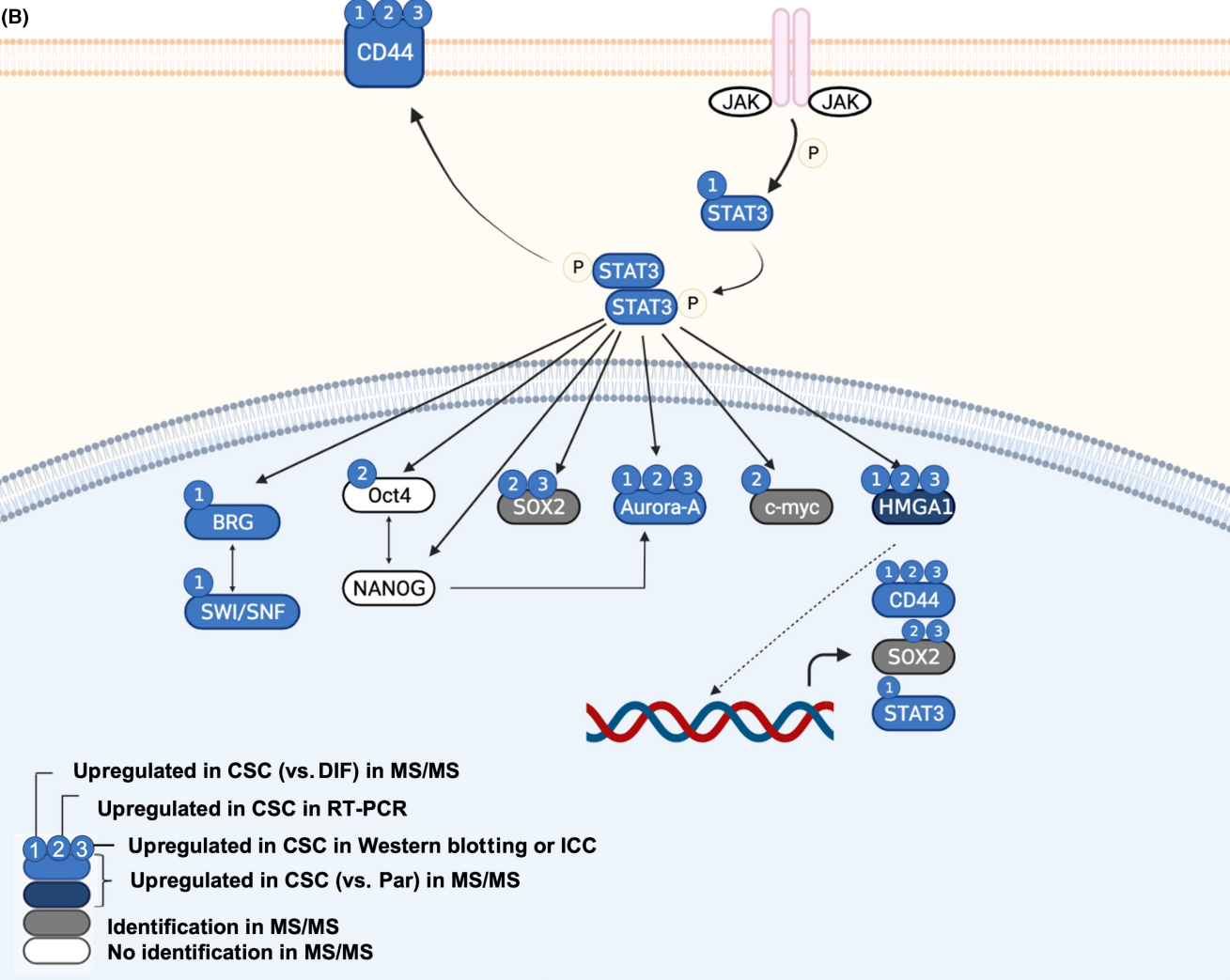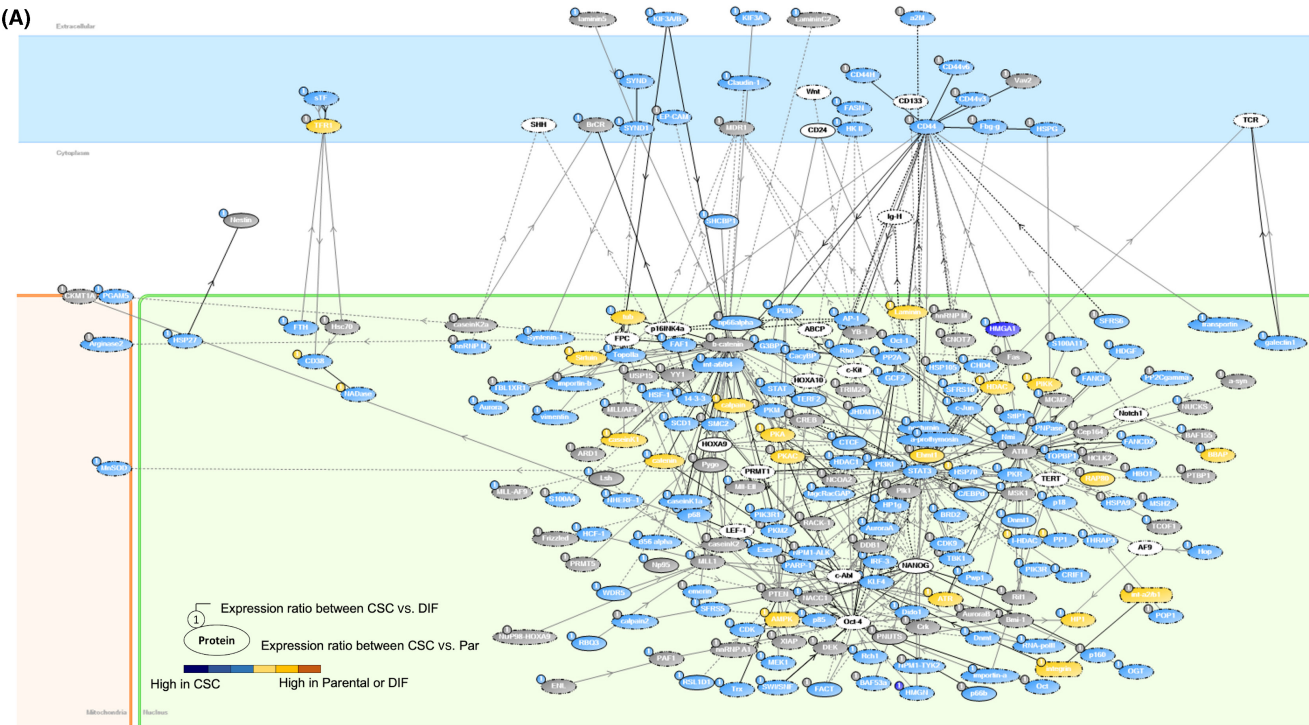| Rank	KeyMolnet pathway	Score	p value
Pathways upregulated in KKU-055-CSC			
1	Spliceosome assembly	54.838	3.11E-17
2	Condensin signaling pathway	41.917	2.41E-13
3	Aurora signaling pathway	26.553	1.02E-08
4	BET family signaling pathway	24.69	3.69E-08
5	Transcriptional regulation by high mobility group protein	20.135	8.68E-07
6	BRCA signaling pathway	19.992	9.59E-07
7	Transcriptional regulation by SREBP	19.086	1.80E-06
8	Kinesin family signaling pathway	17.975	3.88E-06
9	Transcriptional regulation by RB/E2F	17.461	5.54E-06
10	Nucleophosmin signaling pathway	16.426	1.14E-05
11	Arginine methylation	16.23	1.30E-05
12	ATM/ATR signaling pathway	15.604	2.01E-05
13	PARP signaling pathway	14.984	3.09E-05
14	ING signaling pathway	14.815	3.47E-05
15	Topo II signaling pathway	14.63	3.94E-05
16	TACC signaling pathway	14.252	5.13E-05
17	Sirtuin signaling pathway	14.225	5.22E-05
18	CDK signaling pathway	13.901	6.54E-05
19	Transcriptional regulation by Kaiso	13.76	7.21E-05
20	HAT signaling pathway	13.384	9.36E-05
Pathways downregulated in KKU-055-CSC			
1	Lipoprotein metabolism	30.307	7.53E-10
2	Spliceosome assembly	25.517	2.08E-08
3	Integrin family	25.273	2.47E-08
4	Sphingolipid signaling pathway	20.827	5.37E-07
5	Integrin signaling pathway	16.887	8.25E-06
6	ARF family signaling pathway	16.845	8.50E-06
7	Sphingoglycolipid degradation	15.776	1.78E-05
8	HDAC signaling pathway	14.763	3.60E-05
9	VHL signaling pathway	13.398	9.27E-05
10	2-Hydroxyglutarate signaling pathway	12.321	1.96E-04
11	Nicotinic acetylcholine receptor signaling pathway	11.877	2.66E-04

the proteomics (Figure S2). The extracted network indicated that HMGA1 modulates the expression of CD44, SOX2, and STAT3 as a transcriptional factor and also has associations with stem cell factors, including BRG, Oct4, SWI/SNF, c-myc, and CD44 via activation of STAT3 (Figure 7B). This result suggested that the HMGA1-STAT3-Aurora A network regulates stemness maintenance of CSC by controlling stem cell factors.

3.6 | High mobility group A1 signaling pathway regulates stemness maintenance and chemoresistance of CCA-CSC

Our proteomics data suggested the association of HMGA1 with stemness maintenance of CCA-CSC. Western blotting and immunofluorescence showed that HMGA1 is highly expressed in KKU-055-CSC and drastically reduced in KKU-055-DIF and parental KKU-055 cells (Figure 8A). To investigate the role of HMGA1 in CCA-CSC, we silenced HMGA1 expression in KKU-055-CSC using specific siRNA. After siHMGA1 treatment, the expression of HMGA1 in KKU-055-CSC was significantly decreased compared with that of siControl (Figure 8B). The cell proliferation was dramatically increased (Figure 8C). The morphology is slightly changed by increasing the adherent activity to the culture dish (Figure S3). Moreover, we found that the knockdown of HMGA1 leads to the reduction of stem cell markers SOX2 and CD44 in KKU-055-CSC (Figure 8B). Furthermore, KKU-055-CSC treated with siHMGA1 became significantly more sensitive against 5-FU, cisplatin, and gemcitabine than the siControl-treated cells (Figure 8D). These results suggested the role of HMGA1 in stemness maintenance and chemoresistance of CCA-CSC.

3.7 | Aurora signaling pathway involves cell viability of CCA-CSC

In addition to HMGA1, the Aurora signaling pathway is also enriched in KKU-055-CSC (Table 2). Western blot analysis and immunofluorescence confirmed that Aurora A is highly expressed in KKU-055-CSC compared to the KKU-055-DIF and parental KKU-055 (Figure 8E). To investigate the role of the Aurora signaling pathway, five US FDA-approved drugs targeting Aurora A activity were used to treat KKU-055-CSC and compared with the parental cells. After 72 h of the treatments, Aurora A inhibitors showed significantly higher inhibitory effects on the cell viability of KKU-055-CSC than the parental cell (Figure 8F,G). Moreover, we have analyzed the combined effects of the knockdown of HMGA1 and Aurora A inhibitors. After pretreatment with siHMGA1 or siControl for 24 h, CSC and parental cells were treated with the desired concentration of Aurora A inhibitors for 48 h. The results showed that the knockdown of HMGA1 could sensitize the effect

(A)

Expression ratio between CSC vs. DIF

Protein — Expression ratio between CSC vs. Par

High in CSC   High in Parental or DIF

(B)

Upregulated in CSC (vs. DIF) in MS/MS

Upregulated in CSC in RT-PCR

Upregulated in CSC in Western blotting or ICC

Upregulated in CSC (vs. Par) in MS/MS

Identification in MS/MS

No identification in MS/MS

FIGURE 7 Network analysis of proteins upregulated in cholangiocarcinoma stem-like cells (CSC). (A) Network analysis was undertaken in KeyMolnet software using 1123 proteins upregulated in KKU-055-CSC were used as the input for analysis. (B) The enriched signaling pathway is based on high mobility group A1 (HMGA1) and Aurora A. The protein interactions were defined as follows: a solid line with the arrow (direct binding or activation), a solid line with the arrow and stop (direct inactivation), a solid line without the arrow (complex formation), a dashed line with the arrow (transcriptional activation), and a dashed line with arrow and stop (transcriptional repression). ICC, immunocytochemistry; MS/MS, tandem mass spectrometry.
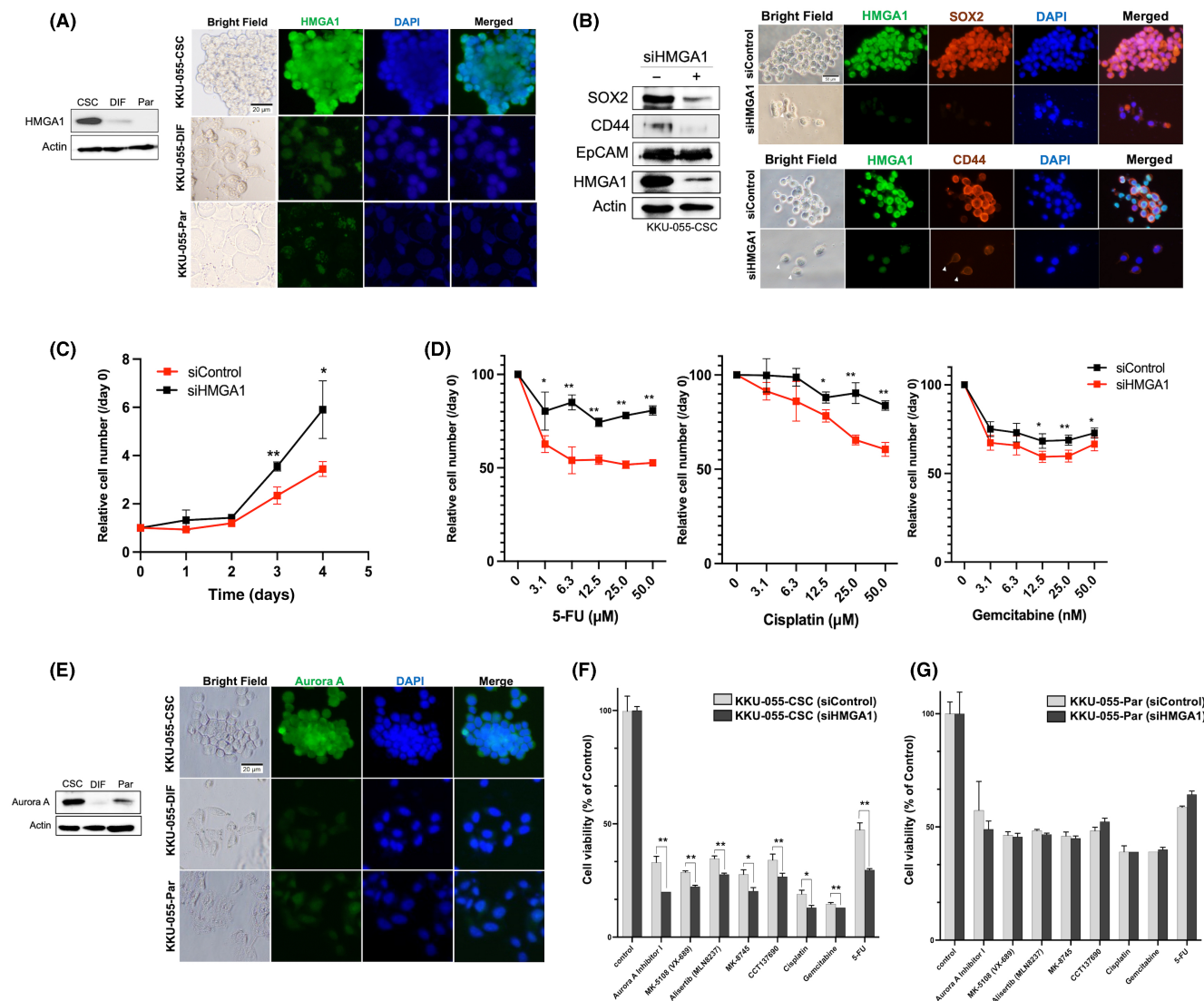
FIGURE 8 Functional analysis of high mobility group A1 (HMGA1) in cholangiocarcinoma cancer stem cells (CSC). (A) Western blotting and immunocytofluorescence were used to determine the high mobility group A1 (HMGA1) expression (green). The nucleus (blue) was stained by DAPI. Scale bar, 20 μm. (B) KKU-055-CSC was treated with 50 pmole of siHMGA1 and compared to siControl. Immunofluorescence measured expressions of HMGA1, SOX2, and CD44. Scale bar, 50 μm. (C) Proliferation assay by CCK-8 and (D) drug sensitivity against 5-fluorouracil (5-FU), cisplatin, and gemcitabine. (E) Western blotting and immunocytofluorescence of Aurora A (green). Scale bar, 20 μm. (F, G) Cell viability was measured by CCK-8 after combined treatment with siHGMA1 and drugs. *$p < 0.05$, **$p < 0.01$. DIF, 10% FCS-induced differentiation form; EpCAM, epithelial cell adhesion molecule; Par, parental KKU-055.

of Aurora A inhibitors in KKU-055-CSC, while this sensitized effect was not observed in parental cells (Figure 8F,G). These findings suggest the potential of combined suppression of HMGA1 and Aurora A for improvement of CCA treatment by targeting CCA-CSC.

3.8 | In silico analysis of *HMGA1* and *Aurora A* in CCA tissues

The mRNA expression of *HMGA1* and *AURKA* in human CCA tissues ($n=36$) were compared, in silico, with normal counterparts ($n=9$)

using the TCGA dataset on the GEPIA online server (http://gepia.cancer-pku.cn/). The expression of *HMGA1* in CCA tissues was significantly higher than in normal tissues (Figure 9A). Kaplan–Meier survival analysis showed that the higher expression of *HMGA1* in human CCA tissues is associated with poor overall survival of patients (Figure 9B). In addition, the *AURKA* level in CCA tissues was found to be positively correlated to *HMGA1* with a Pearson index (R) of 0.73 (*p* value <0.001) (Figure S4). These data suggest the importance of *HMGA1* and *AURKA* in CCA.

4 | DISCUSSION

Cancer stem cells are a minor population of tumor cells discovered as the main factor contributing to tumor development and progression; CSCs are proposed to be an effective target for cancer treatment. Here, we successfully established a cell line-derived CCA stem-like cell, KKU-055-CSC, representing a CSC clone useful for further in vitro and in vivo studies. The cells exhibited CSC phenotypes, including expression of stem cell markers, drug resistance, multilineage differentiation, and tumor formation. In addition, the proteome analysis followed by functional assays revealed the role of HMGA1 and Aurora A in stemness maintenance and chemoresistance of CCA-CSC.

Cancer stem-like cells can be obtained from several sources by many methods.[9,12,26,27] In this study, we isolated the cancer stem-like cells from the CCA cell line using the protocol modified from our previous studies.[15,18] This protocol is practical and simple; just culturing the primary cancer cells or cell lines in specific stem cell media to produce the stem-like cells that can maintain their characteristics in the long term. To authenticate that the isolated cells could be a representative CSC model, several CSC phenotypes should be shown through various in vitro and in vivo experiments.[28–31] In our study, the KKU-055-CSC exhibited CSC phenotypes, such as expression of CSC markers, multilineage differentiation, chemoresistance, and in vivo tumor formation.

The previous studies about CCA stem cells were mainly performed in the short-term culturable CSC-like/spheroid cells or the CSC marker-positive adherent cancer cells.[32,16,32,33] The long-term culturable CCA-CSC clone has never been successfully established; the KKU-055-CSC is the first long-term culturable sphere-forming CCA-CSC clone. However, similar characteristics and marker expression were observed between KKU-055-CSC and those cells. To characterize the CCA-CSC properties of KKU-055-CSCs, we undertook all experiments using the sphere form of KKU-055-CSC and compared it to the FCS-induced differentiation and parental KKU-055 cells. We found that FCS can induce the monolayer attachment of KKU-055-CSC to the culture plate, which is related to the reduction of stem cell marker expression, as shown in Figure 5D.

Cancer stem cell factors/markers regulate stem cell phenotypes,[33] and their suppression could weaken the capacity of CSCs.[34–36] Many CSC markers have been reported for CCA, including ALDH, CD44, CD44v9, CD90, CD133, CD147, EpCAM, and SOX2.[16,32,33] High expression of these CSC markers is associated with poor clinical outcomes in CCA patients.[37] Overexpression of CD44, CD44v6, CD44v8–10, and EpCAM increases the predictability of postoperative CCA recurrence.[32] CD44v9 was reported to induce stem-like phenotypes and enhance CCA progression through the Wnt/β-catenin signaling pathway.[35] In our study, KKU-055-CSC showed a high expression of CSC markers, including CD38, CD44, CD147, SOX2, EpCAM, KLF4, *Oct3/4*, *c-myc*, and *OLG2*. The functional analysis showed that KKU-055-CSC gains the ability on chemoresistance. Supporting this function, our proteomics data showed that KKU-055-CSC expressed a high level of proteins related to multidrug resistance, including ALDH3A1, ALDH1A1, and ATP binding cassette (ABC) transporters. A high level of ALDH expression was reported to associate with the high migratory capacity and gemcitabine resistance of CCA cells.[34] Taken together, our data agree with the previous reports that CD44, CD147, SOX2, EpCAM, Oct3/4, and ALDH could be the potential CSC markers applicable as a target for treating CCA in the future.[16,32,33]

Collectively, our data showed that the KKU-055-CSC is potentially a representative CCA stem-like cell. However, it is known that the population of CSCs are heterogenous; the different CSC clones with different degree of stemness could show different phenotypes and aggressiveness. Thus, KKU-055-CSC might be a particular
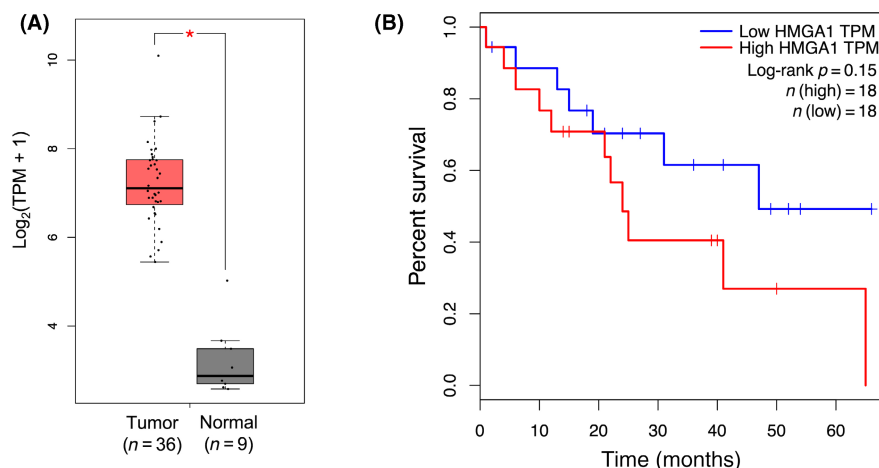
FIGURE 9 Expression of *HMGA1* in human cholangiocarcinoma (CCA) tissues. (A) *HMGA1* mRNA expression in CCA tissues (red bar) compared with normal (gray bar) was analyzed using The Cancer Genome Atlas dataset in GEPIA. *$p < 0.05$. (B) Survival analysis was undertaken using the Kaplan–Meier plot and log-rank test. TPM, transcripts per million.

subgroup of CCA-CSCs. For a better understanding of CSCs of CCA, more CSC-like clones with different phenotypes and degrees of stemness should be isolated and characterized.

Our global proteome analysis revealed the distinct protein expression pattern among KKU-055-CSC, KKU-055-DIF, and parental KKU-055 cells. We found the upregulation of the integrin signaling pathway in KKU-055-DIF and the parental KKU-055 compared with KKU-055-CSC, suggesting the involvement of this signaling pathway during CSC differentiation. Our finding agrees with the previous reports that the integrin signaling is enhanced during CSC differentiation and could serve as a target niche for CSC differentiation.[14,15]

The transcriptional regulation pathway by HMGA was extracted as one of the most enhanced networks in CSC and dramatically declined after differentiation. These results suggested the role of HMGA signaling in the stemness maintenance of CCA stem cells. The HMGA proteins, including HMGA1 and HMGA2, are chromatin architectural proteins interacting with the transcriptional types of machinery to change chromatin structure and regulate the transcription of many genes.[38] It is highly expressed in embryonic stem cells and some adult stem cells, such as hematopoietic and intestinal stem cells, indicating their fundamental role in self-renewal and differentiation in the stem cells.[38] Overexpression of HMGA1 could enhance the expression of *OCT4*, *NANOG*, *SOX2*, and *C-myc* in human embryonic stem cells.[39,40] The HMGA proteins were also overexpressed in many cancer types,[41] including CCA. Our in silico analysis also showed the overexpression of HMGA1 in human CCA tissues, and its high expression was associated with poor survival of CCA patients. In breast cancer, HMGA proteins were found to play a critical role in epithelial–mesenchymal transition.[42] In CSCs, the function of HMGA protein is not yet clearly understood. Network analysis using proteomics data shows HMGA1 and stem cell factor-related proteins (e.g., SOX2, CD44, CD133, EpCAM, KLF4, Nanog, OCT4, OCT1, and SWI/SNF) are associated through STAT3 activation. Signal transducer and activator of transcription 3 was determined to be a downstream target of HMGA1. The HMGA1 binds to the *STAT3* promoter *and activates* the expression level of STAT3 in leukemic cells.[43] Our results indicate that the expression of STAT3 is higher in CSC conditions than in DIF and is not expressed in parental cells (Figure S2). The network analysis in this study suggested that STAT3 regulates the expression of HMGA1 in a feed-forward manner, controlling the expression of STAT3 itself through HMGA1 regulation, which could drive a stem-like cell state of CCA-CSCs. Moreover, our results showed that HMGA1 regulates drug resistance of CCA-CSC. The involvement of HMGA1 in chemoresistance was also found in colon cancer[44,45] and glioblastoma.[46] This evidence suggested the general function of HMGA1 in controlling stemness maintenance and chemoresistance of CSCs.

In addition, in this study, the Aurora signaling pathway was highly enriched in CCA-CSCs. Aurora kinase A (Aurora A) is a serine/threonine kinase that plays an essential role in many steps in cell biology during meiosis.[47] In glioma stem cells, Aurora A regulates self-renewal and tumorigenicity by interacting with AXIN and disrupting the AXIN/GSK3b/β-catenin destruction complex, resulting in the activation of Wnt signaling.[48] Moreover, Aurora A can translocate to the nucleus, which enhances breast cancer stem cell phenotype by activating the MYC promoter.[49] We showed that the treatment of Aurora A inhibitors could reduce the cell viability of both CCA-CSC and parental CCA cells. Interestingly, the suppression of HMGA1 can enhance the Aurora A inhibitor effects, specifically higher in CSC, suggesting the important role of HMGA1 and Aurora A in CCA-CSC. Information on the relationship between HMGA1 and Aurora A is very limited. Our study might be the first to identify the relationship between HMGA1 and Aurora A in CSC. Using TCGA/GEPIA database analysis, we found a strong correlation between *HMGA1* and Aurora A (*AURKA*) mRNA levels in human CCA.

In conclusion, our findings show that HMGA1-AuroraA, possibly through STAT3-related pathways, is the key regulator in the maintenance of CSC-like features in CCA stem cells. Targeting these molecules could be a promising new strategy for CSC-eradication therapeutics; however, further study will be needed to clarify the exact mechanism.

CONFLICT OF INTEREST STATEMENT

Yoshihiro Komohara is currently an Editorial Board Member of *Cancer Science*. The other authors have no conflict of interest. All authors had full access to all of the data in the study and had final responsibility for the decision to submit for publication.

ETHICS STATEMENTS

Approval of the research protocol by an institutional reviewer board: N/A.

Informed consent: N/A.

Registry and registration no. of the study/trial: N/A.

Animal studies: The animal study was approved by the Animal Experiment Committee of Kumamoto University, Japan.

ORCID

Atit Silsirivanit https://orcid.org/0000-0002-5777-3843
Yoshihiro Komohara https://orcid.org/0000-0001-9723-0846
Norie Araki https://orcid.org/0000-0001-9987-6229

REFERENCES

1. Sripa B, Pairojkul C. Cholangiocarcinoma: lessons from Thailand. *Curr Opin Gastroenterol*. 2008;24:349-356.
2. Lee KJ, Yi SW, Cha J, et al. A pilot study of concurrent chemoradiotherapy with gemcitabine and cisplatin in patients with locally advanced biliary tract cancer. *Cancer Chemother Pharmacol*. 2016;78:841-846.
3. Sripa B, Seubwai W, Vaeteewoottacharn K, et al. Functional and genetic characterization of three cell lines derived from a single tumor of an *Opisthorchis viverrini*-associated cholangiocarcinoma patient. *Hum Cell*. 2020;33:695-708.
4. Kawamoto M, Umebayashi M, Tanaka H, et al. Combined gemcitabine and metronidazole is a promising therapeutic strategy for cancer stem-like cholangiocarcinoma. *Anticancer Res*. 2018;38:2739-2748.
5. Luvira V, Eurboonyanun C, Bhudhisawasdi V, et al. Patterns of recurrence after resection of mass-forming type intrahepatic Cholangiocarcinomas. *Asian Pac J Cancer Prev*. 2016;17:4735-4739.
6. Batlle E, Clevers H. Cancer stem cells revisited. *Nat Med*. 2017;23:1124-1134.
7. Klonisch T, Wiechec E, Hombach-Klonisch S, et al. Cancer stem cell markers in common cancers—therapeutic implications. *Trends Mol Med*. 2008;14:450-460.
8. Klemba A, Purzycka-Olewiecka JK, Wcislo G, et al. Surface markers of cancer stem-like cells of ovarian cancer and their clinical relevance. *Contemp Oncol (Pozn)*. 2018;22:48-55.
9. Jariyal H, Gupta C, Bhat VS, Wagh JR, Srivastava A. Advancements in cancer stem cell isolation and characterization. *Stem Cell Rev Rep*. 2019;15:755-773.
10. Pastrana E, Silva-Vargas V, Doetsch F. Eyes wide open: a critical review of sphere-formation as an assay for stem cells. *Cell Stem Cell*. 2011;8:486-498.
11. Masciale V, Grisendi G, Banchelli F, et al. Isolation and identification of cancer stem-like cells in adenocarcinoma and squamous cell carcinoma of the lung: a pilot study. *Front Oncol*. 2019;9:1394.
12. Rao GH, Liu HM, Li BW, et al. Establishment of a human colorectal cancer cell line P6C with stem cell properties and resistance to chemotherapeutic drugs. *Acta Pharmacol Sin*. 2013;34:793-804.
13. Matsuda K, Sato A, Okada M, et al. Targeting JNK for therapeutic depletion of stem-like glioblastoma cells. *Sci Rep*. 2012;2:1-11.
14. Narushima Y, Kozuka-Hata H, Koyama-Nasu R, et al. Integrative network analysis combined with quantitative phosphoproteomics reveals transforming growth factor-beta receptor type-2 (TGFBR2) as a novel regulator of glioblastoma stem cell properties. *Mol Cell Proteomics*. 2016;15:1017-1031.
15. Niibori-Nambu A, Midorikawa U, Mizuguchi S, et al. Glioma initiating cells form a differentiation niche via the induction of extracellular matrices and integrin alphaV. *PLoS One*. 2013;8:e59558.
16. Cardinale V, Renzi A, Carpino G, et al. Profiles of cancer stem cell subpopulations in cholangiocarcinomas. *Am J Pathol*. 2015;185:1724-1739.
17. Correnti M, Raggi C. Stem-like plasticity and heterogeneity of circulating tumor cells: current status and prospect challenges in liver cancer. *Oncotarget*. 2017;8:7094-7115.
18. Putthisen S, Silsirivanit A, Panawan O, et al. Targeting alpha2,3-sialylated glycan in glioma stem-like cells by Maackia amurensis lectin-II: a promising strategy for glioma treatment. *Exp Cell Res*. 2021;410:112949.
19. Ohta K, Kawano R, Ito N. Lactic acid bacteria convert human fibroblasts to multipotent cells. *PLoS One*. 2012;7:e51866.
20. Laemmli UK. Cleavage of structural proteins during the assembly of the head of bacteriophage T4. *Nature*. 1970;227:680-685.
21. Okada S, Vaeteewoottacharn K, Kariya R. Application of highly immunocompromised mice for the establishment of patient-derived xenograft (PDX) models. *Cell*. 2019;8:1-15.
22. Akaboshi S, Watanabe S, Hino Y, et al. HMGA1 is induced by Wnt/beta-catenin pathway and maintains cell proliferation in gastric cancer. *Am J Pathol*. 2009;175:1675-1685.
23. Shaffer LG, McGowan-Jordan J, Shmid M. *An International System for Human Cytogenetic Nomenclature*. Karger Medical and Scientific Publishers; 2013.
24. Masuda T, Ishihama Y. Sample preparation for shotgun proteomics by using phase transfer surfactants. *Proteome Lett*. 2016;1:95-100.
25. Okuda S, Watanabe Y, Moriya Y, et al. jPOSTrepo: an international standard data repository for proteomes. *Nucleic Acids Res*. 2017;45:D1107-D1111.
26. Ghanei Z, Jamshidizad A, Joupari MD, Shamsara M. Isolation and characterization of breast cancer stem cell-like phenotype by Oct4 promoter-mediated activity. *J Cell Physiol*. 2020;235:7840-7848.
27. Palmini G, Zonefrati R, Mavilia C, et al. Establishment of cancer stem cell cultures from human conventional osteosarcoma. *J Vis Exp*. 2016;116:e53884.
28. Alisi A, Cho WC, Locatelli F, Fruci D. Multidrug resistance and cancer stem cells in neuroblastoma and hepatoblastoma. *Int J Mol Sci*. 2013;14:24706-24725.
29. Phi LTH, Sari IN, Yang YG, et al. Cancer stem cells (CSCs) in drug resistance and their therapeutic implications in cancer treatment. *Stem Cells Int*. 2018;2018:5416923.
30. Raggi C, Correnti M, Sica A, et al. Cholangiocarcinoma stem-like subset shapes tumor-initiating niche by educating associated macrophages. *J Hepatol*. 2017;66:102-115.
31. Wang M, Xiao J, Shen M, et al. Isolation and characterization of tumorigenic extrahepatic cholangiocarcinoma cells with stem cell-like properties. *Int J Cancer*. 2011;128:72-81.
32. Padthaisong S, Thanee M, Namwat N, et al. Overexpression of a panel of cancer stem cell markers enhances the predictive capability of the progression and recurrence in the early stage cholangiocarcinoma. *J Transl Med*. 2020;18:64.
33. McGrath NA, Fu J, Gu SZ, Xie C. Targeting cancer stem cells in cholangiocarcinoma (review). *Int J Oncol*. 2020;57:397-408.
34. Chen MH, Weng JJ, Cheng CT, et al. ALDH1A3, the major aldehyde dehydrogenase isoform in human cholangiocarcinoma cells, affects prognosis and gemcitabine resistance in cholangiocarcinoma patients. *Clin Cancer Res*. 2016;22:4225-4235.
35. Suwannakul N, Ma N, Midorikawa K, et al. CD44v9 induces stem cell-like phenotypes in human cholangiocarcinoma. *Front Cell Dev Biol*. 2020;8:417.
36. Yan Y, Li Z, Kong X, et al. KLF4-mediated suppression of CD44 signaling negatively impacts pancreatic cancer stemness and metastasis. *Cancer Res*. 2016;76:2419-2431.
37. Gu MJ, Jang BI. Clinicopathologic significance of Sox2, CD44 and CD44v6 expression in intrahepatic cholangiocarcinoma. *Pathol Oncol Res*. 2014;20:655-660.
38. Parisi S, Piscitelli S, Passaro F, Russo T. HMGA proteins in stemness and differentiation of embryonic and adult stem cells. *Int J Mol Sci*. 2020;21:1-17.
39. Shah SN, Kerr C, Cope L, et al. HMGA1 reprograms somatic cells into pluripotent stem cells by inducing stem cell transcriptional networks. *PLoS One*. 2012;7:e48533.

40. Yanagisawa BL, Resar LM. Hitting the bull's eye: targeting HMGA1 in cancer stem cells. *Expert Rev Anticancer Ther.* 2014;14:23-30.

41. Sepe R, Piscuoglio S, Quintavalle C, et al. HMGA1 overexpression is associated with a particular subset of human breast carcinomas. *J Clin Pathol.* 2016;69:117-121.

42. Pegoraro S, Ros G, Piazza S, et al. HMGA1 promotes metastatic processes in basal-like breast cancer regulating EMT and stemness. *Oncotarget.* 2013;4:1293-1308.

43. Belton A, Xian L, Huso T, et al. STAT3 inhibitor has potent antitumor activity in B-lineage acute lymphoblastic leukemia cells overexpressing the high mobility group A1 (HMGA1)-STAT3 pathway. *Leuk Lymphoma.* 2016;57:2681-2684.

44. D'Angelo D, Mussnich P, Rosa R, Bianco R, Tortora G, Fusco A. High mobility group A1 protein expression reduces the sensitivity of colon and thyroid cancer cells to antineoplastic drugs. *BMC Cancer.* 2014;14:851.

45. Kim DK, Seo EJ, Choi EJ, et al. Crucial role of HMGA1 in the self-renewal and drug resistance of ovarian cancer stem cells. *Exp Mol Med.* 2016;48:e255.

46. Puca F, Tosti N, Federico A, et al. HMGA1 negatively regulates NUMB expression at transcriptional and post transcriptional level in glioblastoma stem cells. *Cell Cycle.* 2019;18:1446-1457.

47. Li M, Gao K, Chu L, Zheng J, Yang J. The role of Aurora-a in cancer stem cells. *Int J Biochem Cell Biol.* 2018;98:89-92.

48. Xia Z, Wei P, Zhang H, et al. AURKA governs self-renewal capacity in glioma-initiating cells via stabilization/activation of beta-catenin/Wnt signaling. *Mol Cancer Res.* 2013;11:1101-1111.

49. Zheng F, Yue C, Li G, et al. Nuclear AURKA acquires kinase-independent transactivating function to enhance breast cancer stem cell phenotype. *Nat Commun.* 2016;7:10180.

SUPPORTING INFORMATION

Additional supporting information can be found online in the Supporting Information section at the end of this article.